Reinforcement of Polylactic Acid / Poly Butylene Adipate-co-Terephthalate blends by starch addition: A coupled computational and experimental study

Paolino Caputo [a], Pietro Calandra [b,*], Alessandro Pecchia [b], Bernardino Tirri [b], Francesco Mercuri [c], Fabrizio Lo Celso [d], Flaviano Testa [e], Valeria. Loise [a], Cesare Oliviero Rossi [a]

[a] Department of Chemistry and Chemical Technologies, University of Calabria, UdR INSTM della Calabria, Via P. Bucci, Cubo 14/D, Rende (CS) 87036, Italy
[b] CNR-ISMN National Council of Research, Strada provinciale 35 D n.9, 00010 Montelibretti (RM), Italy
[c] DAIMON Lab - CNR-ISMN, Via P. Gobetti 101, 40129 Bologna, Italy
[d] Università degli Studi di Palermo, Dipartimento di Fisica e Chimica, Viale delle Scienze Ed. 17, Palermo, Italy
[e] Dipartimento di ingegneria Informatica, Modellistica, Elettronica e Sistemistica, Università della Calabria, Cubo 44A-Via Pietro Bucci, 87030 Arcavacata di Rende (CS), Italy

GRAPHICAL ABSTRACT
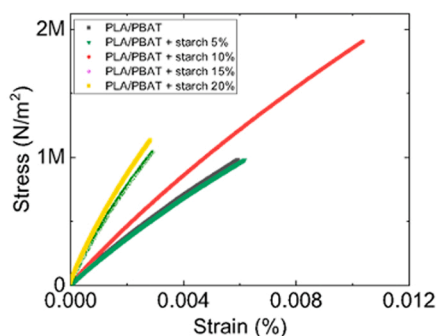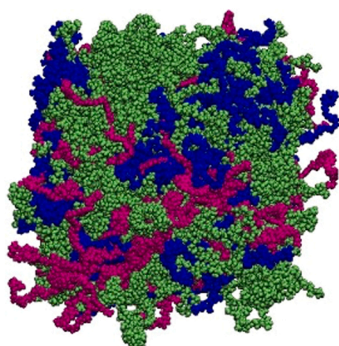
ARTICLE INFO

ABSTRACT

Poly Lactic Acid / Poly Butylene Adipate-co-Terephthalate blends are used as packaging green materials since they constitute hydrophilic and biodegradable plastic. With the aim of improving the mechanical characteristics of such blends as biodegradable packaging materials for food products the addition of starch has been considered. In silico test performed by classical molecular dynamics highlighted that the addition of starch can reinforce the polymeric structure via starch-polymer interactions, suggesting that starch can be a suitable material to be added to the Poly Lactic Acid / Poly Butylene Adipate-co-Terephthalate blend to obtain more resistant packaging materials. Experimental analysis of the mechanical properties of the polymeric blend containing different amounts of starch confirmed what foreseen by MD, highlighting an increase of Young modulus and glass transition as a function of added starch. The coupled theoretical/experimental approach constitutes added value of the present work, furnishing important data on the reinforcement of the packaging material performances and a molecule-based interpretation and comprehension of the observed phenomenon.

1. Introduction

The unsustainability of the use of materials from non-renewable resources and the compounding problem of environmental pollution have made the research of biodegradable materials an important focus for scientists.

In particular, the scarcity of petroleum-based materials, as well as the recently ascertained unsustainability of their use, caused a breaking down of conventional, not biodegradable, plastics so a need for their replacement with bio-based materials is strongly emerging.

In this ambit, a common substitute biomaterial is Polylactic Acid (PLA). PLA is prepared from lactic acid, widely available via biological fermentation of starches, sugars and other forms of biomass [1,2]. PLA has high transparency and elastic modulus, which are appealing physico-chemical properties for the development of disposable products. For this reason, it has been found how to thermoplastically process PLA like conventional plastics to produce disposable cutlery, bottles, cups and films [3–5]. The biodegradability of PLA is a huge advantage as it degrades into carbon dioxide, water and other small molecules thus making the composting process relatively simple[6,7]. See Scheme 1 for the PLA molecular structure.

Unfortunately, PLA has also some limiting characteristics: low impact strength, low heat resistance and high tendency to hydrolyze. For this reason, it is important to modify PLA to improve its physico-chemical properties.

A very effective and practical way of achieving this is the addition of Poly Butylene Adipate-co-Terephthalate (PBAT). PBAT is a commonly known hydrophilic and biodegradable plastic: it can undergo degradation when subjected to either soil or composting conditions [8]. PBAT is a nicely flexible material, with a high elongation at break. For this reason, it has been used to produce blown film and its associated membrane products [9–12].

A previous study investigated the compatibility, crystallization and tensile properties of different proportions of PLA/PBAT blends obtained via a melt-blending process and the results demonstrated that PBAT effectively increased the toughness of PLA[13]. The carbonyl in the structure of PBAT (see PBAT molecular structure in Scheme 1) makes it compatible with PLA during the melt-blending process [14–18].

After that work, the PBAT has been shown to modify the brittleness and decrease the rate of crystallization of PLA [19,20].

In this framework, we want to further improve the mechanical characteristics of PLA/PBAT blends to obtain more resistant biodegradable packaging materials for food products by ad-hoc addition of other suitable materials. Keeping attention of renewable, environmentally friendly, biodegradable substances, raw materials like starches, lignin, chitosan, keratin, collagen, cellulose and gelatin, need to be considered since they have emerged as suitable starting materials for the synthesis of bio-based polymers. Starch, which is a naturally abundant material, is one of the most common biopolymers in this category and has a high potential for the production of eco-friendly products for mass commercial use. Its primary use is mainly as a food ingredient but, more recently, it has been identified as a suitable alternative in industrial processes such as paper, textile and pharmaceutical and even construction fields [21–24].

With the aim to test starch as possible reinforcing element to improve the PLA/PBAT mechanical properties, we describe an integrated theoretical/experimental approach based on a qualitative *in-silico* study to foresee the structural effects of starch addition to a PLA/PBAT matrix,
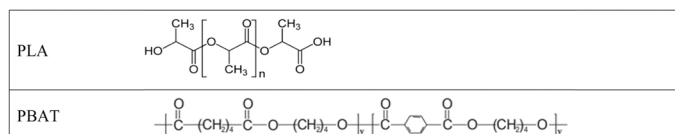
followed by the experimental check of the increased performance in real samples. The theoretical approach is based on classical Molecular Dynamics (MD) simulations and, on the basis of their results, PLA/PBAT blends have been prepared with various amount of starch and studied by Dynamic Mechanical Analysis (DMA).

It must be underlined that the final goal of the MD simulations was not to show the differences between theoretically predicted quantities and the experimentally measured ones but, rather, to in silico investigate the influence of the starch in different conditions, to see whether the changes induced by its presence can suggest a real reinforcement of the PLA/PBAT polymer blend.

The simultaneous use of the two complementary, theoretical and experimental, approaches is of added value and will furnish a deep comprehension of the reinforcement of PLA/PBAT blends with starch for packaging purposes at the microscopic level.

2. Computational details

PLA and PBAT polymer chains were built in 2D by means of Marvin [25] which provides CML coordinates file format. OPLS-AA parameter force field for the PLA and PBAT were then generated from CML coordinates using the web server service PolyParGen [26–29]. The Amylose chain structure and subsequent force field parameter were obtained by means of CHARMM-GUI web-based service [30] and CHARMM36 force field parameters were used [31].

The number of monomers in the model polymer chains for PLA, PBAT and Amylose were 40, 9 (for both blocks) and 60 respectively.

For the molecular dynamics (MD) simulation, a cubic box of 54 nm was filled initially with 200 PLA chains and 68 PBAT ones using PackMol software [32]; the same initial configuration was used for the ternary system in which 9 Amylose chains were added.

MD simulations were performed by GROMACS 2021.4 version [33–35].

For both systems the same protocol was applied. A minimization run was carried out to avoid possible overlapping. While pressure was kept constant at 1 bar (time step used was 1fs) the systems were equilibrated for 200 ns at $T = 600$ K, for 100 ns at $T = 400$ K, for 100 ns at $T = 800$ K and then cooled down to $T = 100$ K at a cooling rate of 10 K/ns with a step of 100 K. Simulated systems were then heated up to $T = 800$ K at a heating rate of 10 K/ns with a step of 100 K, and equilibrated for 200 ns at $T = 800$ K. From this point a run of 10 ns at $T = 800$ K was done for statistical purposes saving the trajectory every 10 ps. The systems were cooled down slower from $T = 800$ K to $T = 600$ K at a cooling rate of 5 K/ns and a cooling step of 20 K. A 300 ns equilibration run was done at $T = 600$ K followed by a 10 ns statistical one. The same cooling procedure was applied going from 600 K to 400 K and then a 600 ns equilibration was applied at 400 K followed by a 10 ns statistical one. The different equilibration time were strongly dependent on the temperatures; during the runs the RMSD of the systems were checked.

Radii of gyration (Rg), radial distribution functions (g(r)), and the density have been statistically analysed using the MDanalysis toolkit [36,37], whereas radial pair distribution functions (RPDFs) have been computed using the VMD software [38,39].

Estimation of the Glass Temperature (Tg) was performed by progressive cooling form 800 K to 100 K (step 20 K, cooling rate 5 K/ns) and then by evaluating the intersection point of the extrapolated trends in the lower (100–250 K) and higher (500–800 K) ranges.

3. Experimental part

3.1. Sample preparation

Poly Lactic Acid (PLA) was purchased by Sigma Aldrich and used as received. It is a solid and biodegradable polyester synthesized from lactic acid monomer via ring opening polymerization. The Mw is around 60000 g/mol. Poly Butylene Adipate-co-Terephthalate (PBAT, Ecoflex

Scheme 1. Molecular structure of PLA and PBAT.

FBX 1200), was supplied by BASF Corporation (Germany). Poly(45% butylene adipate-co-55% butylene terephthalate) with a melt flow index of 3.3–6.6 g per 10 min (at 190 °C), density of 1.25–1.27 g cm^{-3}, the weight-average molecular weight of 142 000 g/mol.

PLA/PBAT blends were prepared by using a mechanical stirrer (IKA RW20, Germany). The melt compounding was performed at 160 °C and a screw speed of 60 rpm. The PLA/PBAT weight ratio was fixed at 70/30.

Ternary blends comprising PBAT, PLA and Starch were prepared by mixing the PLA/PBAT blends at 70/30 relative wt% with starch until the desired starch wt% (X) was obtained. Firstly, PLA/PBAT blends were melted at 160 °C and mixed for 4 min (IKA RW20, Germany), then starch was added and mixed for another 4 min

Preliminary Scanning Electron Microscopy investigation showed that the samples were homogeneous at the nanoscale, with discontinuities appearing only at low magnification, at a micrometer-scale (bulk).

3.2. Material characterization

The mechanical and viscoelastic behaviour of the blends was determined using dynamic mechanical analysis (DMA50 from Metravib, Acoem) in a Tension model configuration. The samples dimension was 30 mm length, 10 mm height and the thickness of 1 mm. The results were analysed with DYNATEST software. A temperature scan was performed on blends from 25 to 100 °C at a heating rate of 1 °C/min. It was verified previously that the deformation was in the linear domain. The frequency was fixed at 1 Hz.

DMA measurements consist in applying a sinusoidal force/deformation to a blend structure and measuring its deformation/force, or even applying a constant force/deformation and measuring its creep/relaxation modulus. Based on these measurements, DMA can determine several properties of a material, like modulus and viscosity [40].

The modulus is reported over the test as a complex quantity E * (ω): the real part, E′(ω), called as storage or elastic modulus, corresponds to the elastic response and it represents the material's ability to return or store energy. It may represent shear, tensile or flexural modulus, depending on the operational mode chosen to be used. On the other hand, the imaginary part, E″(ω), known as loss or viscous modulus, is associated with the viscous response, corresponding to ability of the material under investigation to dissipate energy. The loss factor tanδ is given by the ratio E″(ω)/E′(ω), where δ is the phase angle between stress and strain resulting from the viscoelastic nature of the material [41].

Young's modulus was determined by force vs displacement curves, the value is calculated from the slope of the initial part of a stress-strain curve, is similar conceptually to the storage modulus, they are not the same. Just as shear, bulk and compressive moduli for a material will differ, Young's modulus will not have the same value as the storage modulus.

Samples were subjected to a speed rate of 0.2 mm min^{-1}, applying a controlled force (from 0.1 N up to 25 N) until the sample breaks at room temperature. This test is repeated 3 times for each sample. The values are reported as the mean values of the sets of measurements and the uncertainties are the corresponding standard deviations. All experiments were performed at 25 °C.

Thermogravimetric analysis (TGA) was performed using a DSC-TGA STA409C analyzer.

(Netzsch-Gerätebau GmbH, Selb, Germany) from 40 to 500 °C at a heating rate of 5 °C in static air.

4. Results and discussion

4.1. Molecular dynamics (MD)

Kernel Density Estimations (KDE) depicted in Fig. 1 show the distributions of the computed radii of gyration for the investigated materials. On the first glance, population distributions of both PLA and PBAT in the binary blend slightly vary as simulation temperatures rise. This effect is significant for the PLA, where the trimodal distribution observed at 400 K vanishes. Like the PLA, for the PBAT the Rg distributions softly converge in a bimodal distribution at 800 K, with <Rg> values of 36.6 Å, 35.4 Å, and 38.7 Å at 400 K, 600 K, and 800 K, respectively (Table 1). Our statistical results indicates that the starch marginally alters the multidimensional structure of polymers, which is consistent with the immiscibility and thus with the interactions of hydrophobic polymers and hydrophilic starch [42]. Indeed, the introduction of starch slightly impacts the Rg distributions of both PLA and PBAT compounds, as well as the general trend observed for the mean Rg value (<Rg>) of PBAT.

Fig. 1 and Table 1 show that the largest density probabilities are located in the region spanning from first to third quartiles. Although distributions are characterized by multimodal nature, they softly converge toward a bimodal behaviour. Unlike the binary blend, the <Rg> of PBAT molecules in the ternary mixture decreases at 400 K, indicating that the introduction of starch at this temperature leads compact PBAT structures (Table S.1).

To better show the change of <Rg> values with temperature, a linear regression of the data has been performed. The best lines are reported in Fig. 2 for the PLA and PBAT in the binary and ternary blends.

The slopes of the linear equations were examined to derive valuable physical insights into the behaviour of the polymer blends in terms of <Rg> . Specifically, the slope of the PLA equation in the binary blend was 0.007, while that of PBAT was 0.005, indicating a slightly higher temperature sensitivity of PLA compared to PBAT in the binary blend. In the ternary blend, the slope of the PLA equation was 0.004, while that of PBAT was 0.012, signifying that the addition of potato starch had a great impact, causing a change of the <Rg> behaviour of both PLA and PBAT upon temperature changes. Hence, the slopes of PBAT for the ternary blend is steeper than those of the binary blend, indicating that the <Rg> changes more rapidly with temperature for the ternary blend. In other words, this suggests that the addition of starch leads to a more temperature-sensitive chain PBAT structure in the polymer blend. On the other hand, PLA seems to become more insensitive to temperature changes if starch is added. It can be hypothesized that a preferential interaction between starch and PLA with stabilization of the latter, can hold, with a consequent reduction of hindrances on PBAT.

The impact of starch on the PLA and PBAT distances in the blend is shown in Fig. 3, where the Radial Pair Distribution Functions (RPDFs) of the various samples are reported.

Briefly, RPDF represents the average distribution of atoms around any given atom within the system.

For both blends, the first shoulder is located at approximately 5 Å, while the second shoulder is situated around 9 Å. Although no significant shift is observed for the shoulders, there is an increase in their intensity, indicating a slightly higher probability of locating atoms of PLA molecules around PBAT molecules and vice versa. Furthermore, at elevated temperatures, the RPDFs exhibit a sigmoidal character in the curves, with a decreased intensity gap between them. These results suggest that the effect of starch is less pronounced under high-temperature conditions.

Then, at low temperatures, the potato starch is affecting the interaction between the polymers as evidenced by the intensity of the RPDF peaks for the ternary blend. Here, the greater effect on PBAT in the ternary blend suggests that the potato starch has a greater impact on the 3D PBAT chains, leading to a more compact conformation. This effect may be related to the different molecular structures of PLA and PBAT, as well as the interaction between the potato starch and the polymers. It is noteworthy that at elevated temperatures, the distinction in the RPDFs intensity between the binary and ternary blends becomes less discernible, which is consistent with the <Rg> previously reported. Actually, starch presence in the systems lowers the thermal agitation effects: actually, in presence of starch, temperature exerts its effects only at short ranges (distances < 8 Å) leaving almost unaltered the structure at longer
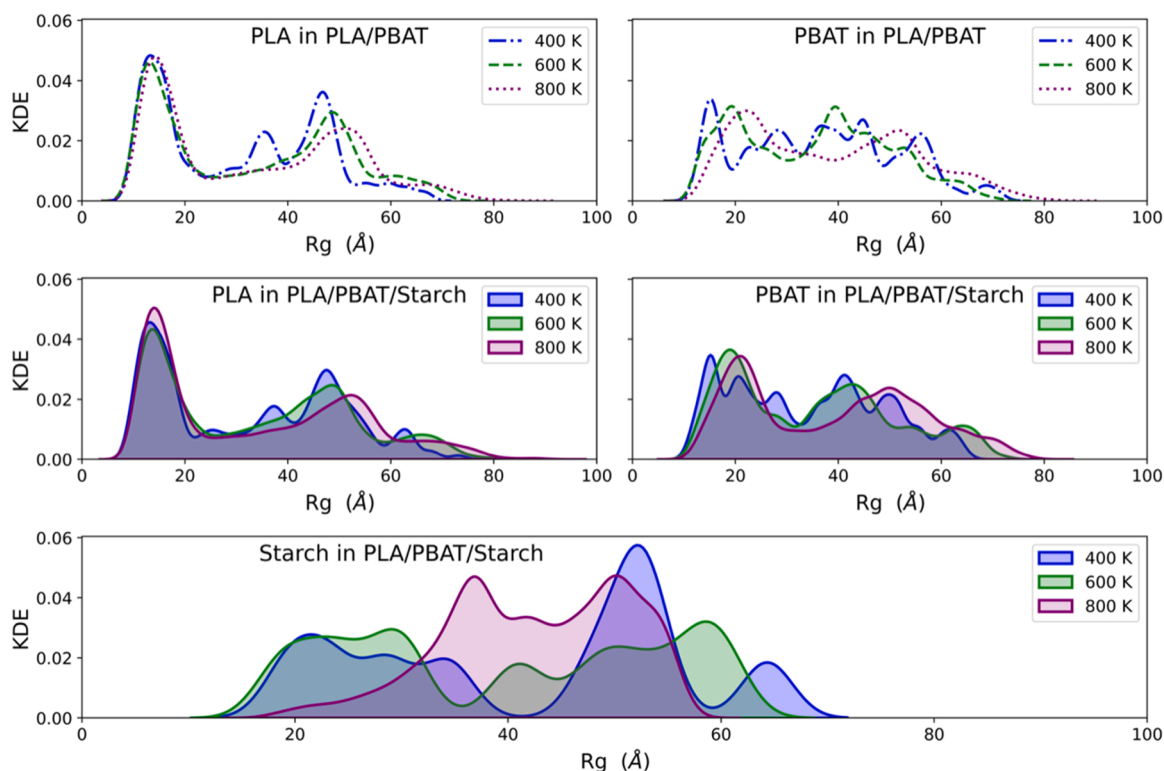
Fig. 1. KDE plots of the radii of gyration of: PLA (upper left panel) and PBAT (upper right panel) in the binary blend, PLA (central left panel) and PBAT (central right panel) in the ternary blend, and starch (bottom panel) in the ternary blend.

Table 1

Statistics for the binary and ternary blends at different temperatures (T). Mean value ($< Rg >$), standard deviations (σ), minimum radius of gyration (*min*), percentiles (25%, 50%, 75%) and maximum value (*max*).

T	Statistics	PLA/PBAT		PLA/PBAT/starch		
		PLA	PBAT	PLA	PBAT	Starch
	$< Rg >$	30.86	36.65	32.66	34.04	41.75
	σ	15.82	15.02	17.30	14.59	14.78
	min	9.09	12.62	9.35	11.91	19.33
	25%	15.05	23.86	15.19	20.40	28.55
	50%	31.53	36.74	33.44	34.19	48.19
	75%	45.27	46.86	47.60	45.43	52.39
400 K	max	67.61	72.50	74.17	65.85	64.69
	$< Rg >$	33.24	35.43	34.12	35.36	39.84
	σ	17.77	14.40	18.381	15.86	14.70
	min	8.35	11.10	8.12	10.97	17.33
	25%	15.12	21.46	15.74	20.49	25.82
	50%	33.61	36.85	34.29	35.35	40.94
	75%	48.57	46.16	48.54	46.18	53.96
600 K	max	74.46	72.79	85.68	73.82	61.58
	$< Rg >$	33.71	38.79	34.08	38.96	42.56
	σ	18.44	16.27	19.71	16.96	8.46
	min	8.57	11.26	8.58	10.35	17.44
	25%	15.58	23.76	15.16	22.19	36.51
	50%	32.41	37.61	31.26	40.41	42.86
	75%	49.93	51.75	51.01	52.42	49.89
800 K	max	87.31	84.90	92.76	80.14	57.66

distances. This reinforces the finding that starch contributes in making more robust the whole structure, as an overall, final, effect of the interplay of the various interactions involved, sometimes characterizing chemical complex systems [43] like those under investigation.

Fig. 4 shows the radial distribution functions at different simulation temperatures for the investigated blends. At 400 K, the RDFs of both mixtures are characterised by sharp and narrow peaks, suggesting a certain degree of rigidity in terms of molecular packaging. As shown by

Fig. 4, thermic effects have a significant impact on RPDFs. Therefore, structured peaks at 400 K tend to disappear as the temperature rises. Increasing temperature at 600 K, the PLA peaks decrease in intensity and RDFs have broad shape in both blends. Hence, the centres of mass distances are uniform throughout the simulation box. It should be noted that the g(r) profiles obtained at 800 K are similar to those obtained at 600 K, and, generally, the melting temperatures of the biodegradable binary and ternary blends are lower than 600[44–46].

Fig. 5 depicts the density histogram for the investigated systems.

In the PLA/PBAT blend, the density at 400 K fluctuates around 1173 Kg/m^3, see Fig. 5 for density distributions for the various samples. As expected, increasing simulation temperatures results in a decrease in density (Table 2). Here, the peaks are approximately 1011 Kg/m^3 and 852 Kg/m^3 at 600 K and 800 K respectively. When the starch is added, at 400 K, the densities of binary blend increases at any temperature: the histograms show a peak around 1192 Kg/m^3 at 400 K, while at 600 K and 800 K the histograms reveal that the mean densities are around 1033 Kg/m^3 and 873 Kg/m^3, respectively.

As a results of MD analysis, it can be concluded that starch addition is expected to reinforce the PLA/PBAT structure, making it more compact.

This clue is reinforced by estimation of the Glass Temperature (Tg) performed by progressive cooling form 800 K to 100 K. As it can be seen from Fig. 6, a change of slope in the density-temperature profile is observed around 380 K in PLA/PBAT blend, whereas this inflection is shifted to 400 K in PLA/PBAT/starch system, showing an increase of 20 degrees upon starch addition. The increase in Tg is another, self-consistent, indication that the structure is reinforced when starch is added.

4.2. Dynamic mechanical analysis (DMA)

In Fig. 7, measured stress-strain curves are reported, which enable the identification of the maximum strain that the sample can bear before breaking. Maximum strain values are also reported in Fig. 7 (right
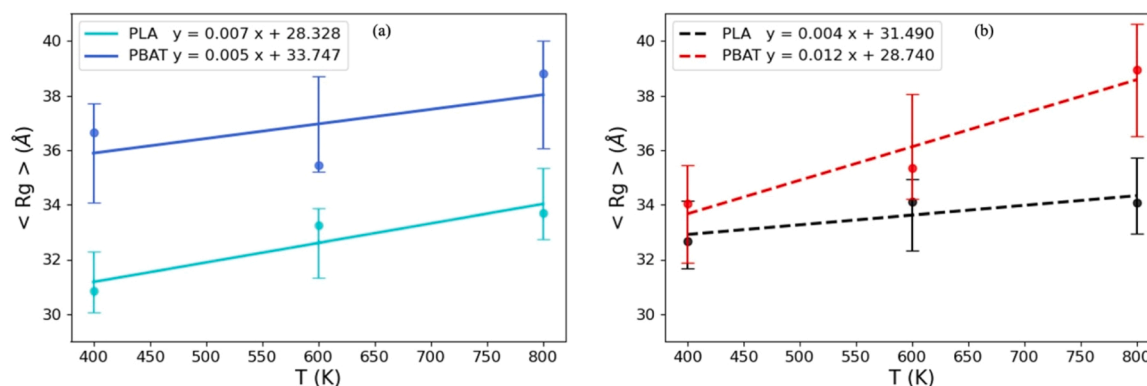
Fig. 2. Plot of the <Rg> as a function of temperature for the binary (left panel, solid line) and ternary (right panel, dashed lines) blends.
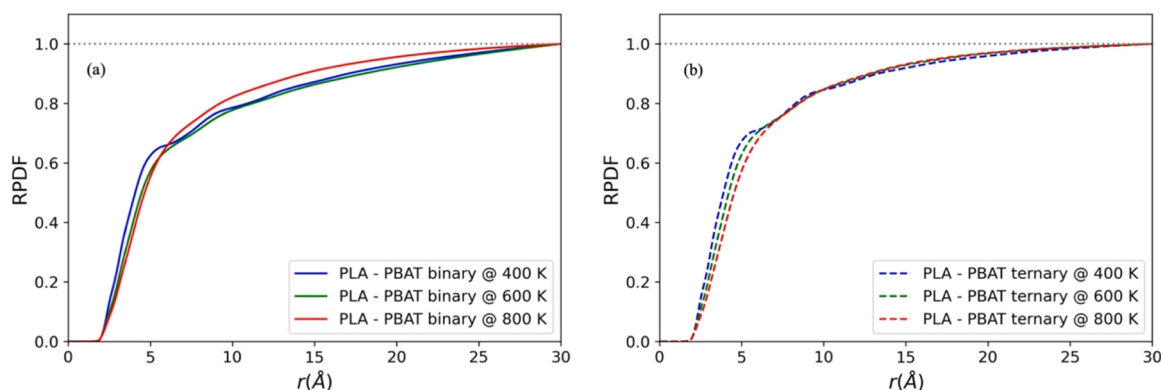

Fig. 3. Normalised RPDFs of PLA and PBAT polymers in the binary (a) and ternary (b) blends.

panel). From the average slope of the stress-strain curve it is possible also to derive the Young modulus (see Table 3). The same table also reports the viscosity values, which share the same trend of the young moduli. The plot in Fig. 7 and the values reported in Table 3 show that, upon starch addition, the young modulus and the viscosities increases monotonically as a consequence of the increased rigidity offered by the polymer-starch interactions highlighted in the MD section. For starch contents $\leq 10\%$ this is also highlighted by the increase in the maximum strain that the material can bear prior to rupture. However, further addition of starch causes a parallel, further increase in young modulus and in viscosity, but a decrease in the maximum strain probably due to the occurrence of starch-starch interactions. It can be then concluded that the starch content of 10% appears to be the optimal amount of starch to be added to PLA/PBAT for improving its characteristics.

Further information can be derived from Dynamic mechanical analysis (DMA) as a function of temperature.

Via DMA, a temperature ramp is applied while a small-amplitude linear oscillation is imposed to the sample to measure the dynamic moduli E′, E″, and tan(δ) (tan(δ)=E″/E′).

When heating a polymer from the glassy state it experiences a transition from a hard and brittle material to a softer rubbery material with more viscous properties. This is the glass transition. The glass transition is heavily influenced by such factors as the crystallinity of the polymer, crosslinking, and plasticizers. The glass transition's sensitivity to these factors makes it an ideal parameter to quantify for quality control purposes and to see the influence of these factors on the performance and processing of polymers. The glass transition occurs over a range of temperatures and is not a point or single temperature. It is helpful to define unambiguous points within the transition region to characterize the glass transition which we will refer to as Tg. Often the glass transition is reported as a single temperature but the details of how it was determined are needed to make any quantitative comparison of

two materials.

In our case, Tg was derived by the maximum occurring in the tan(δ) vs. T curve. The method of determining the glass transition points is identical for either extensional or shear deformation and should yield identical results in isotropic materials. The measured Tg is sensitive to the frequency of the oscillation (in this work the experiments were performed at the fixed frequency of 1 Hz) and it is independent of the amplitude within a small region that is easily achievable.

In our conditions, as shown in Fig. 8, the Tg shifts at higher temperatures when the starch in present in the blend for starch $\leq 15\%$. This demonstrates how the starch increases the resistance towards higher temperatures. Also, this finding confirms what has been foreseen by the computational investigation.

However, starch content higher than 15 wt% causes a decrease in Tg. The maximum Tg is therefore observed at starch 15%. This is an important point, and the fact that the maximum is observed at 15 wt% does not contrast the clues from stress-strain curve: If the young modulus and the maximum strain are mechanical characteristics at room temperature, here the evaluation of Tg gives information on the resistance of the material to the temperature. The two kinds of information need to be then considered as complementary for a more global vision of the material.

Further information can be derived from thermogravimetric analysis (TGA). TGA is widely used as a suitable technique to investigate the thermal stability and decomposition of starch & starch-based materials and to determine the content of starch and other components that are generally present in mixtures of starch with artificial and synthetic polymers.

In the Fig. 9 the thermogravimetric profiles for the isolated PLA/PBAT blend, the isolated starch and the PLA/PBAT/starch blend are reported. Thermogravimetric analysis shows that the polymer has no significant weight loss in the 80–160 °C temperature range, which is in
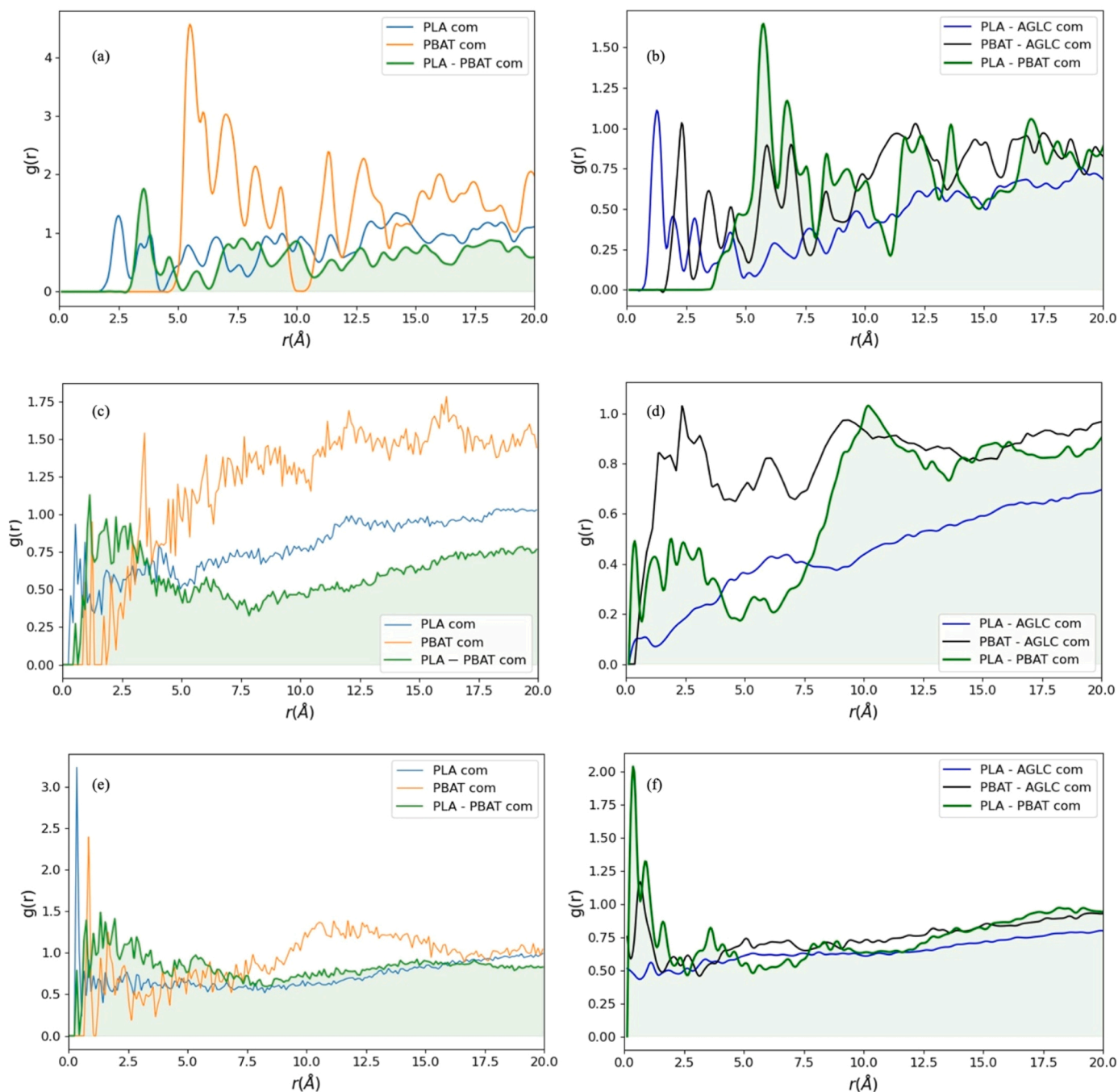
Fig. 4. Radial distribution functions at 400 K (a,b), 600 K (c, d), and 800 K (e,f) for the binary (left panel), and ternary (right panel) blends.

the zone where weight loss due to the presence of water and low-–molecular weight compounds is expected [47,48]. In the same range, the starch-related sample, shows a weight loss of about 13%. The second stage, from 250 to 350 °C, corresponds to loss of hydroxyl groups and depolymerization of carbon chains [49]. Finally, the last stage above 350 °C is due to the carbonization decomposition of raw starch and starch nanocrystals. Thermogravimetric analyses performed on the blends containing different amounts of starch, show an increase in water vapor/low–molecular weight compounds loss obviously due to the increase of starch content. It must be underlined that the samples containing starch were subjected to heating at a temperature of 120 °C in order to allow for the starch-polymer mixing, so the weight loss around 100 °C due to the water vapor and the low –molecular weight compounds loss is not expected. This revealed to occur for samples

containing low starch content (≤10 wt%). However, samples with higher starch percentages (≥15 wt%) showed water vapor/-low–molecular weight loss (see Table 5, where the weight losses at significant and selected temperatures have been reported for all the samples) since the heating time was not enough to completely remove them from the samples.

Fig. 9 reports the experimental curve of a representative starch-containing sample (20 wt%) as compared to the hypothetical curve of an ideal sample at the same starch content (i.e. calculated as 0.8 times the curve PLA/PBAT + 0.2 times the curve starch). As it can be seen from inspection of this comparison, the curve of the real starch-containing sample deviates from the ideal starch-polymer mixing behavior. This is due to starch-polymer interactions. In particular, a reduced loss of water vapor and low–molecular weight compounds in the initial stage
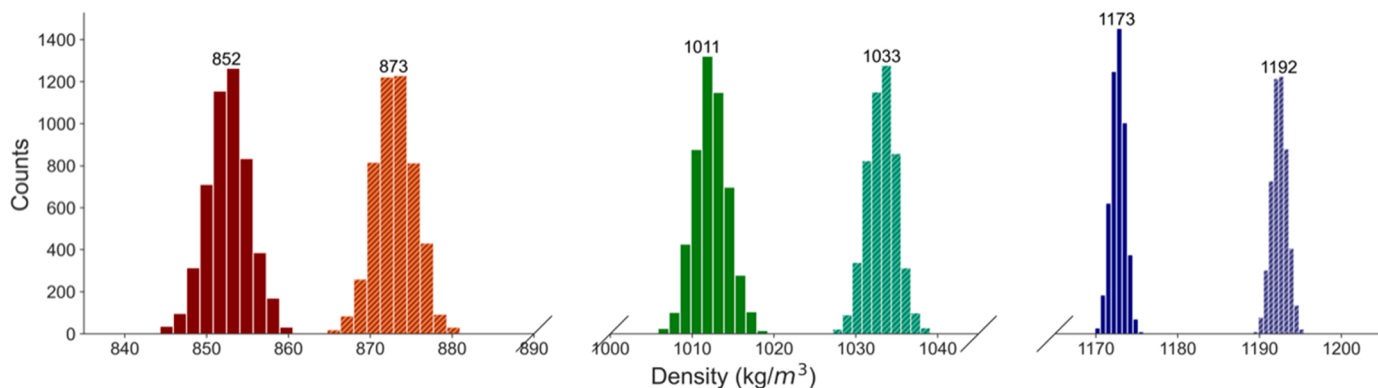
Fig. 5. Density histograms at 800 K (red binary, light red ternary), 600 K (green binary, light green ternary), and 400 K (blue binary, light blue ternary) for the investigated blend.

Table 2
Statistics for the binary and ternary blends at different temperatures (*T*). Density mean value ($< \rho >$) in Kg/m^3, standard deviations (σ).

T		PLA/PBAT	PLA/PBAT/starch
	$< \rho >$	1172.7	1192.4
400 K	σ	0.86	0.93
	$< \rho >$	1012	1033
600 K	σ	2.0	1.8
	$< \rho >$	853	873
800 K	σ	2.6	2.4

Table 3
young modulus and viscosities of the various samples.

Sample	Young Modulus (N/m^2) $\pm$ 0.02	Viscosity 25 °C (Pa) $\pm$ 2%
PLA/PBAT	1.64	$5.3 \cdot 10^6$
PLA/PBAT + 5% Starch	1.71	$5.3 \cdot 10^6$
PLA/PBAT + 10% Starch	1.82	$6.0 \cdot 10^6$
PLA/PBAT + 15% Starch	3.49	$1.22 \cdot 10^8$
PLA/PBAT + 20% Starch	3.88	$1.47 \cdot 10^8$

Table 4
Glass transition.

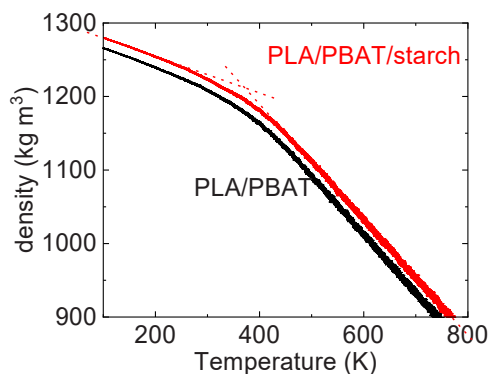| Sample	Tg (°C)
Polymer	61.1
Polymer + 10 Starch	64.5
Polymer + 15 Starch	85.3
Polymer + 20 Starch	80.5

Fig. 6. Density as a function of temperature for the studied samples.

up to about 120 °C is shown. This can be due to the heating used for polymer-starch homogenization, but it cannot be excluded that specific starch-polymer interactions could stabilize the material. In addition, a more resistance to the second stage degradation, occurring in the 250 -

350 °C interval, and corresponding to loss of hydroxyl groups and depolymerization of carbon chains, seems to occur. This is certainly the consequence of the interactions between the polymer blend and the starch, reasonably via its hydroxyl groups. Finally, above 350 °C, the starch carbonization seems to occur at lower temperature. It can be argued that starch-polymer interactions could weaken the intra-molecular starch chain-chain interactions diminishing their stabilization. After all, the phenomenon where the establishment of *inter*molecular interactions weakens the *intra*molecular ones has already been seen
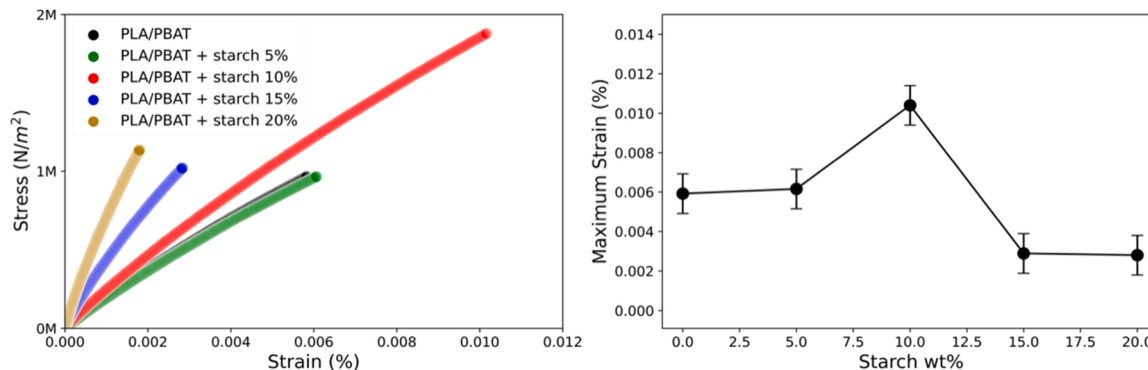

Fig. 7. left panel: stress-strain plot for PLA/PBAT/starch composites at various starch wt%. Right panel: maximum strain beared by the composites under investigation as a function of starch wt%.
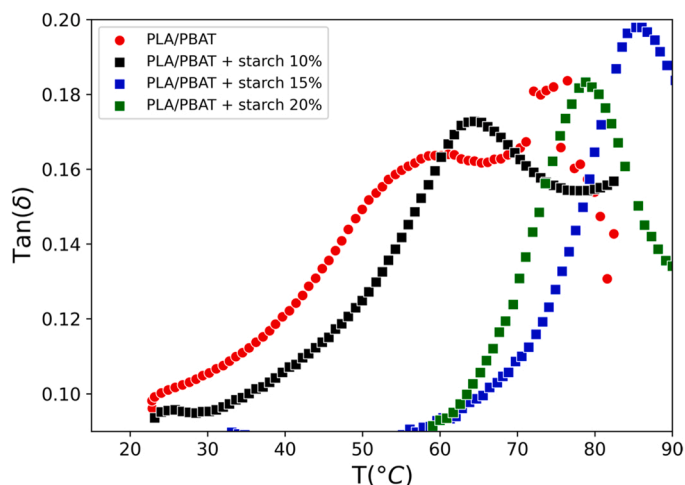
Fig. 8. tan(δ) in the range 25–90 °C at 1 Hz and with a 1 °C/min ramp.
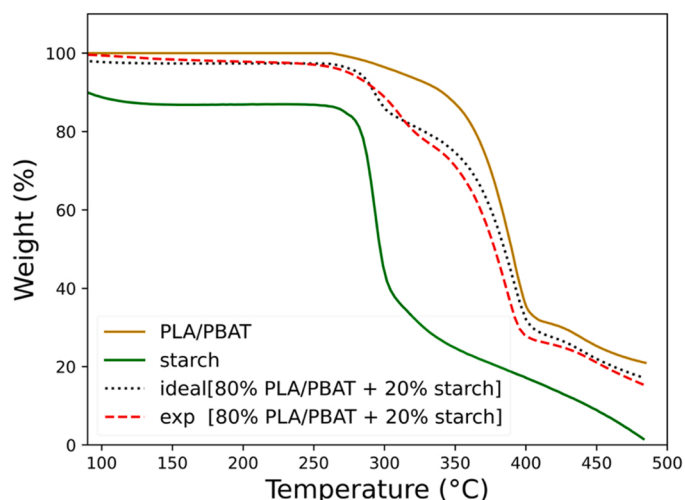

Fig. 9. The thermogravimetric profiles for the PLA/PBAT polymer blend, starch and the polymer blend containing starch at 20% (red line experimental data, black line calculated line see text for details).

Table5
Weight Loss in the 130–160 °C range.

Sample	Weight Loss (%) 130 °C	Weight Loss (%) 140 °C	Weight Loss (%) 150 °C	Weight Loss (%) 160 °C
PLA/PBAT	0	0	0	0
starch	12.9	13.1	13.1	13.2
PLA/PBAT + starch 5%	0	0	0	0
PLA/PBAT + starch 10%	0	0	0	0
PLA/PBAT + starch 15%	1.2	1.4	1.5	1.7
PLA/PBAT + starch 20%	1.3	1.5	1.6	1.7

in polymeric materials[50]. However, this is a mere hypothesis needing confirmation from further experimental structural studies. In this ambit we can indicate sophisticated light and synchrotron X-ray and neutron scattering experiments [51]as valid tools. In conclusions, TGA measurements confirms the occurrence of interactions between starch and the polymer blend, giving a certain compaction of the overall structure, in agreement with all the previous results.

5. Conclusions

Starch was successfully used as a green material to improve the mechanical characteristics of Poly Lactic Acid (PLA) / Poly Butylene Adipate-co-Terephthalate (PBAT) blends for biodegradable packaging purposes. This modification was *in-silico* suggested by Molecular Dynamics (MD) simulations, which highlighted that the addition of starch can reinforce the polymeric structure via starch-polymer interactions. Experiments of Dynamic Mechanical Analysis on PLA/PBAT blends containing different amounts of starch confirmed what foreseen by MD, highlighting an increase of Young modulus together with a parallel embrittlement as a function of added starch. The optimal amount of starch has been therefore individuated: 10 wt%. This composition also exhibits the maximum strain bearable before rupture. For starch contents higher than 10% wt/wt, a maximum in the glass transition temperature occurs (starch 15 wt%), but the progressive embrittlement worsens the mechanical characteristics. The coupled theoretical/experimental approach constitutes added value of the present work.

In conclusion, the work has proven that a green, cheap and highly available material like starch can be of added value in improving biodegradable packaging materials. In addition, this material can be found in waste material from other industrial activities, fostering a circular economy mechanism with undiscussed environmental benefits [52,53]. So, as future perspective we cannot but indicating the research on the use of starch- containing wastes for packaging improvements. In this sense, the present work has furnished important data and a molecule-based interpretation/comprehension of the phenomenon involved.

CRediT authorship contribution statement

Testa Flaviano: Data curation, Formal analysis, Investigation. **Oliviero Rossi Cesare:** Conceptualization, Supervision, Validation. **Loise Valeria:** Visualization, Writing – review & editing. **Caputo Paolino:** Data curation, Validation, Visualization. **Calandra Pietro:** Formal analysis, Funding acquisition, Project administration, Writing – original draft, Writing – review & editing. **Pecchia Alessandro:** Conceptualization, Investigation. **Tirri Bernardino:** Formal analysis, Visualization. **Mercuri Francesco:** Conceptualization, Investigation, Methodology. **Lo Celso Fabrizio:** Data curation, Investigation, Methodology, Resources, Software.

Declaration of Competing Interest

The authors declare that they have no known competing financial interests or personal relationships that could have appeared to influence the work reported in this paper.

Data availability

Data will be made available on request.

References

[1] B. Kamm, P.R. Gruber, M. Kamm, Biorefineries–industrial processes and products, Ullmann's Encycl. Ind. Chem. (2016) 1–38, https://doi.org/10.1002/14356007.l04_l01.pub2.
[2] K. Madhavan Nampoothiri, N.R. Nair, R.P. John, An overview of the recent developments in polylactide (PLA) research, Bioresour. Technol. 101 (2010) 8493–8501, https://doi.org/10.1016/j.biortech.2010.05.092.

[3] H. Tsuji, Poly(Lactic Acid). in: Bio-Based Plastics, John Wiley & Sons, Ltd, 2013, pp. 171–239, https://doi.org/10.1002/9781118676646.ch8.

[4] R. Auras, B. Harte, S. Selke, An overview of polylactides as packaging materials, Macromol. Biosci. 4 (2004) 835–864, https://doi.org/10.1002/mabi.200400043.

[5] R.A. Auras, S.P. Singh, J.J. Singh, Evaluation of oriented poly(lactide) polymers vs. existing PET and oriented PS for fresh food service containers, Packag. Technol. Sci. 18 (2005) 207–216, https://doi.org/10.1002/pts.692.

[6] A. Södergård, M. Stolt, Properties of lactic acid based polymers and their correlation with composition, Prog. Polym. Sci. 27 (2002) 1123–1163, https://doi.org/10.1016/S0079-6700(02)00012-6.

[7] V. Dornburg, A. Faaij, M. Patel, W.C. Turkenburg, Economics and GHG emission reduction of a PLA bio-refinery system—combining bottom-up analysis with price elasticity effects, Resour. Conserv Recycl 46 (2006) 377–409, https://doi.org/10.1016/j.resconrec.2005.08.006.

[8] A. Bher, P.C. Mayekar, R.A. Auras, C.E. Schvezov, Biodegradation of biodegradable polymers in mesophilic aerobic environments, Int J. Mol. Sci. 23 (2022), https://doi.org/10.3390/ijms232012165.

[9] U. Witt, T. Einig, M. Yamamoto, I. Kleeberg, W.-D. Deckwer, R.-J. Müller, Biodegradation of aliphatic–aromatic copolyesters: evaluation of the final biodegradability and ecotoxicological impact of degradation intermediates, Chemosphere 44 (2001) 289–299, https://doi.org/10.1016/S0045-6535(00)00162-4.

[10] Y. Someya, Y. Sugahara, M. Shibata, Nanocomposites based on poly(butylene adipate-co-terephthalate) and montmorillonite, J. Appl. Polym. Sci. 95 (2005) 386–392, https://doi.org/10.1002/app.21333.

[11] Y.-X. Weng, Y.-J. Jin, Q.-Y. Meng, L. Wang, M. Zhang, Y.-Z. Wang, Biodegradation behavior of poly(butylene adipate-co-terephthalate) (PBAT), poly(lactic acid) (PLA), and their blend under soil conditions, Polym. Test. 32 (2013) 918–926, https://doi.org/10.1016/j.polymertesting.2013.05.001.

[12] L. Jiang, M.P. Wolcott, J. Zhang, Study of biodegradable polylactide/poly(butylene adipate-co-terephthalate) blends, Biomacromolecules 7 (2006) 199–207, https://doi.org/10.1021/bm050581q.

[13] J.-T. Yeh, C.-H. Tsou, C.-Y. Huang, K.-N. Chen, C.-S. Wu, W.-L. Chai, Compatible and crystallization properties of poly(lactic acid)/poly(butylene adipate-co-terephthalate) blends, J. Appl. Polym. Sci. 116 (2010) 680–687, https://doi.org/10.1002/app.30907.

[14] Y. Xu, M. Hanna, Preparation and properties of biodegradable foams from starch acetate and poly(tetramethylene adipate-co-terephthalate), Carbohydr. Polym. 59 (2005) 521–529, https://doi.org/10.1016/j.carbpol.2004.11.007.

[15] E. Quero, A.J. Müller, F. Signori, M.-B. Coltelli, S. Bronco, Isothermal cold-crystallization of PLA/PBAT blends with and without the addition of acetyl tributyl citrate, Macromol. Chem. Phys. 213 (2012) 36–48, https://doi.org/10.1002/macp.201100437.

[16] M.-B. Coltelli, I.Della Maggiore, M. Bertoldo, F. Signori, S. Bronco, F. Ciardelli, Poly(lactic acid) properties as a consequence of poly(butylene adipate-co-terephthalate) blending and acetyl tributyl citrate plasticization, J. Appl. Polym. Sci. 110 (2008) 1250–1262, https://doi.org/10.1002/app.28512.

[17] A. Bhatia, R. Gupta, S. Bhattacharya, H. Choi, Compatibility of Biodegradable Poly (lactic acid) (PLA) and Poly (butylene succinate) (PBS) Blends for Packaging Application, Korea Aust. Rheol. J. 19 (2007).

[18] X. Ma, J. Yu, N. Wang, Compatibility characterization of poly(lactic acid)/poly (propylene carbonate) blends, J. Polym. Sci. B Polym. Phys. 44 (2006) 94–101, https://doi.org/10.1002/polb.20669.

[19] S. Gu, K. Zhang, J. Ren, H. Zhan, Melt rheology of polylactide/poly(butylene adipate- co-terephthalate) blends, Carbohydr. POLYM. - CARBOHYD POLYM 74 (2008) 79–85, https://doi.org/10.1016/j.carbpol.2008.01.017.

[20] H. Xiao, W. Lu, J. Yeh, Crystallization behavior of fully biodegradable poly(lactic acid)/poly(butylene adipate-co-terephthalate) blends, J. Appl. Polym. Sci. 112 (2009) 3754–3763, https://doi.org/10.1002/app.29800.

[21] K.K. Sadasivuni, P. Saha, J. Adhikari, K. Deshmukh, M.B. Ahamed, J.-J. Cabibihan, Recent advances in mechanical properties of biopolymer composites: a review, Polym. Compos 41 (2020) 32–59, https://doi.org/10.1002/pc.25356.

[22] A. Kakoria, S. Sinha-Ray, A Review on Biopolymer-Based Fibers via Electrospinning and Solution Blowing and Their Applications, Fibers 6 (2018), https://doi.org/10.3390/fib6030045.

[23] T. Hemamalini, V.R. Giri Dev, Comprehensive review on electrospinning of starch polymer for biomedical applications, Int J. Biol. Macromol. 106 (2018) 712–718, https://doi.org/10.1016/j.ijbiomac.2017.08.079.

[24] A.A. Abe, C. Oliviero Rossi, P. Caputo, Biomaterials and Their Potentialities as Additives in Bitumen Technology: A Review, Molecules 27 (2022), https://doi.org/10.3390/molecules27248826.

[25] ⟨https://marvinjs-demo.chemaxon.com/latest/demo.html⟩, (n.d.).

[26] M. YABE, K. Mori, K. UEDA, M. TAKEDA, Development of PolyParGen Software to Facilitate the Determination of Molecular Dynamics Simulation Parameters for Polymers, J. Comput. Chem., Jpn. -Int. Ed. 5 (2019) n/a, https://doi.org/10.2477/jccjie.2018-0034.

[27] http://polypargen.com/, (n.d.). http://polypargen.com/ (accessed July 1, 2023).

[28] W. Jorgensen, J. Tirado-Rives, Molecular modeling of organic and biomolecular systems using BOSS and MCPRO, J. Comput. Chem. 26 (2005) 1689–1700, https://doi.org/10.1002/jcc.20297.

[29] L. Dodda, I. Cabeza de Vaca, J. Tirado-Rives, W. Jorgensen, LigParGen web server: An automatic OPLS-AA parameter generator for organic ligands, Nucleic Acids Res 45 (2017), https://doi.org/10.1093/nar/gkx312.

[30] S. Jo, T. Kim, V.G. Iyer, W. Im, CHARMM-GUI: A web-based graphical user interface for CHARMM, J. Comput. Chem. 29 (2008) 1859–1865, https://doi.org/10.1002/jcc.20945.

[31] J. Huang, A. MacKerell, CHARMM36 all-atom additive protein force field: Validation based on comparison to NMR data, J. Comput. Chem. 34 (2013), https://doi.org/10.1002/jcc.23354.

[32] L. Martínez, R. Andrade, E.G. Birgin, J.M. Martínez, PACKMOL: A package for building initial configurations for molecular dynamics simulations, J. Comput. Chem. 30 (2009) 2157–2164, https://doi.org/10.1002/jcc.21224.

[33] M.J. Abraham, T. Murtola, R. Schulz, S. Páll, J.C. Smith, B. Hess, E. Lindahl, GROMACS: High performance molecular simulations through multi-level parallelism from laptops to supercomputers, SoftwareX 1–2 (2015) 19–25, https://doi.org/10.1016/j.softx.2015.06.001.

[34] B. Hess, C. Kutzer, D. van der Spoel, E. Lindahl, GROMACS 4: algorithms for Highly Efficient, Load-Balanced, and Scalable Molecular Simulation, J. Chem. Theory Comput. 4 (2008) 435–447, https://doi.org/10.1021/ct700301q.

[35] D. van der Spoel, E. Lindahl, B. Hess, G. Groenhof, A. Mark, H. Berendsen, GROMACS: fast, flexible, and free, J. Comput. Chem. 26 (2005) 1701–1718, https://doi.org/10.1002/jcc.20291.

[36] R. Gowers, M. Linke, J. Barnoud, T. Reddy, M. Melo, S.L. Seyler, J. Domański, D. Dotson, S. Buchoux, I. Kenney, O. Beckstein, MDAnalysis: A Python Package Rapid Anal. Mol. Dyn. Simul. (2016), https://doi.org/10.25080/Majora-629e541a-00e.

[37] N. Michaud-Agrawal, E.J. Denning, T.B. Woolf, O. Beckstein, MDAnalysis: A toolkit for the analysis of molecular dynamics simulations, J. Comput. Chem. 32 (2011) 2319–2327, https://doi.org/10.1002/jcc.21787.

[38] W. Humphrey, A. Dalke, K. Schulten, VMD: Visual molecular dynamics, J. Mol. Graph 14 (1996) 33–38, https://doi.org/10.1016/0263-7855(96)00018-5.

[39] V.M.D. Visual Molecular Dynamics, (n.d.). http://www.ks.uiuc.edu/Research/vmd/. (accessed July 1, 2023).

[40] K.P. Menard, Dynamic Mechanical Analysis: A Practical Introduction, 2nd ed, CRC Press, Boca Raton, 2008.

[41] I.R. Henriques, L.A. Borges, M.F. Costa, B.G. Soares, D.A. Castello, Comparisons of complex modulus provided by different DMA, Polym. Test. 72 (2018) 394–406, https://doi.org/10.1016/j.polymertesting.2018.10.034.

[42] M. Ferrarezi, M. Taipina, L. Silva, M. Gonçalves, Poly(Ethylene Glycol) as a Compatibilizer for Poly(Lactic Acid)/Thermoplastic Starch Blends, J. Polym. Environ. 21 (2012), https://doi.org/10.1007/s10924-012-0480-z.

[43] P. Calandra, D. Caschera, V. Turco Liveri, D. Lombardo, How self-assembly of amphiphilic molecules can generate complexity in the nanoscale, Colloids Surf. A Physicochem Eng. Asp. 484 (2015) 164–183, https://doi.org/10.1016/j.colsurfa.2015.07.058.

[44] J. Ludwiczak, S. Frąckowiak, K. Leluk, Study of Thermal, Mechanical and Barrier Properties of Biodegradable PLA/PBAT Films with Highly Oriented MMT, Materials 14 (2021), https://doi.org/10.3390/ma14237189.

[45] Y. Guo, X. Zuo, Y. Xue, Y. Zhou, Z. Yang, Y.-C. Chuang, C.-C. Chang, G. Yuan, S. K. Satija, D. Gersappe, M.H. Rafailovich, Enhancing Impact Resistance of Polymer Blends via Self-Assembled Nanoscale Interfacial Structures, Macromolecules 51 (2018) 3897–3910, https://doi.org/10.1021/acs.macromol.8b00297.

[46] Q. Ju, Z. Tang, H. Shi, Y. Zhu, Y. Shen, T. Wang, Thermoplastic starch based blends as a highly renewable filament for fused deposition modeling 3D printing, Int J. Biol. Macromol. 219 (2022) 175–184, https://doi.org/10.1016/j.ijbiomac.2022.07.232.

[47] Y. Liu, L. Yang, C. Ma, Y. Zhang, Thermal Behavior of Sweet Potato Starch by Non-Isothermal Thermogravimetric Analysis, Materials 12 (2019), https://doi.org/10.3390/ma12050699.

[48] Y. Liu, L. Yang, Y. Zhang, Thermal behavior and kinetic decomposition of sweet potato starch by non-isothermal procedures, Arch. Thermodyn. 40 (2019) 67–82, https://doi.org/10.24425/ather.2019.130008.

[49] R.A. Shapi'i, S.H. Othman, R.K. Basha, M.N. Naim, Mechanical, thermal, and barrier properties of starch films incorporated with chitosan nanoparticles 11 (2022) 1464–1477, https://doi.org/10.1515/ntrev-2022-0094.

[50] A. Bartolotta, P. Calandra, Indication of Local Phase Separation in Polyimide/Silica Hybrid Polymers, Macromol. Chem. Phys. 211 (2010) 1784–1792, https://doi.org/10.1002/macp.201000110.

[51] D. Lombardo, P. Calandra, M.A. Kiselev, Structural Characterization of Biomaterials by Means of Small Angle X-rays and Neutron Scattering (SAXS and SANS), and Light Scattering Experiments, Molecules 25 (2020), https://doi.org/10.3390/molecules25235624.

[52] F. Casarejos, C.R. Bastos, C. Rufin, M.N. Frota, Rethinking packaging production and consumption vis-à-vis circular economy: A case study of compostable cassava starch-based material, J. Clean. Prod. 201 (2018) 1019–1028, https://doi.org/10.1016/j.jclepro.2018.08.114.

[53] C. Charoenrungrueang, A. Sawettham, S. Ngeoywijit, S. Weesaphen, M. Kosacka-Olejnik, The circular economy practices of the Tapioca Starch Industry in Northeastern Thailand, Sci. J. Pozn. Univ. Technol. 84 (2021).